We appreciate the reviewer' valuable comments and constructive suggestions which help us improve the quality of the manuscript. We have carefully revised the manuscript according to these comments. Point-to-point responses are provided below. The reviewer' comments are in black, our responses are in blue and the corresponding changes in manuscript are in red.

Reviewer #2

This analysis is divided in two parts: first, a comparison of aerosol properties retrieved by inversion code SKYRAD versions 4.2 and 5.0 is performed, based on two years of data for two SKYNET sites. Second, version 5.0 is used to analyze the aerosol characteristics at the two sites. This kind of study is needed for the improvement of the SKYNET network methodology, and also for the improvement of our knowledge of the aerosol characteristics at China. Therefore, it is adequate for this journal.

However, I would recommend to accept the paper after a major revision, mainly related to: adding detail to the text - improving the graphical representations - further discussing the temporal behavior of aerosol at the two sites

The use of English is adequate, although some flaws are pointed out and I would recommend a revision.

Response: Thank you for your valuable comments and constructive suggestions. We have carried out additional experiments and found that the calibration constants in the previous experiments were incorrect, so we corrected them and re-carried out the experiments and numerical tests; some results and figures have been updated and represented in the following response.

We have added more details related to the graphical, climate and major chemical compositions in PM2.5 in the two sites. Some of the new figures and comments about inter-comparisons results between V5.0 and V4.2 have been shown in the following comments. Meanwhile, we have also investigated some parameters linked to the SSA differences between the V5.0 and V4.2, the seasonal variation of aerosol have been discussed combining the possible emission sources and prevailing wind based on more data and references as shown in the following comments.

General comments:

Introduction: Some more background discussion would be welcome. Please add also a few comments about general differences between versions 4.2 and 5.0. Non-sphericity, minimization

technique used, etc, so general readers can learn about these codes.

Response: Non-sphericity particle model are neither included in V4.2 nor V5.0. We have added the comment in the revised manuscript.

V4.2 uses the iterative relaxation method of Nakajima et al. (1983, 1996) to remove the multiple scattering contributions and derive an optimal solution using a statistical regularization method (Turchin and Nozik, 1969) by minimizing the cost function as proposed by Phillips (1962) and Twomey (1963).

V5.0 uses the non-linear maximum likelihood method defined by Rodgers (2000) which was based on the Bayesian theory. The non-linear inversion has a strong dependence on the estimation of the first-guess solution. Version 5.0 uses an a priori SDF of a bimodal log-normal function.

Section 2.1: Please explain the method used for the calibration, and any findings you consider interesting to note, if any (calibration drift, etc).

Response: The Improved Langley (IL) plot method is used in this study to determine the temporal and spectral calibration constants for direct intensity (F0) with accuracy of about 1.0–2.5 %, depending on the wavelength (Nakajima et al., 1996; Campanelli et al., 2004). The calibration by IL plot method is made daily, the variation of F0 due to instrumental drift can be quickly spotted, and then appropriate corrections to data can be applied exactly from the period in which the deviation occurred (Campanelli et al., 2004). We have added the above comments in the revised manuscript.

It is important also to detail the description of the two sites, including a map if possible, to understand aerosol characteristics. -

Response: We have added a map in the revised manuscript to show the locations of the two SKYNET sites in this study as shown in the following figure.

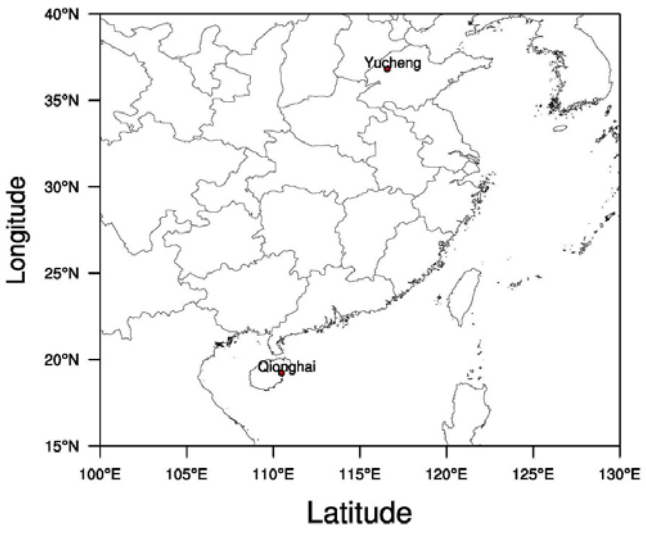

Figure 1: The locations of the two SKYNET sites in the study

In section 2.2 Site description, we have added some more details including monsoon, temperature, and precipitation. We have added the following descriptions in the revised manuscript.

The Qionghai site of SKYNET (19.23°N, 110.46°E, 24 m a.s.l.), which was located in the eastern part of Hainan Island, was mainly influenced by East Asia monsoons and typhoons. During summer, the dominant wind is from south to southeast, summer monsoon from the South China Sea and West Pacific brought most of the annual rainfall to the island (Zhu et al., 2005), whereas the winter monsoon from Inner Mongolia carries dry winds to the area (Zhu et al., 2005; Peel et al., 2007; Yin et al., 2002). Annual average rainfall in Qionghai is estimated about 1653.4 mm. Maximum high temperature occurs in July, with monthly average of 28.6 ^{o}C, monthly lowest temperature occurs in January, with monthly average of 19.1^{o}C (Yin et al., 2002).

The other measurement site in this study was located in rural Yucheng (36.82°N, 116.57°E, 22 m a.s.l.), Shandong Province, China, which is almost in the centre of the North China Plain. The selected site is in an open field surrounded by farmland. The region belongs to semi-humid and temperate monsoon climate zone, characterized by a mean annual temperature of 21^{o}C and mean annual precipitation of 610 mm mainly distributed in summer months (Chen et al., 2012).Yucheng and the surrounding areas are famous for their agriculture (e.g., wheat and corn) and grazing land (e.g., donkeys and chickens). In addition, the site near 20 to 30 km radius located several factories in the production of inorganic and organic fertilizers (Wen et al., 2015), and the application of fertilisers to farmland emitted a great deal of NH3 (Zhao et al., 2012). Meanwhile, Yucheng was located in the downwind of the Beijing-Tianjin-Hebei region, long-distance transport of sources of industrial

pollution and biomass burning contributed significantly to the concentrations of pollutants in Yucheng (Lu et al., 2016).

In addition, based on the results simulated by the Community Multi-scale Air Quality model with the 2D Volatility Basis Set (CMAQ/2D-VBS) (23), we have added the following comments and figure in the revised manuscript to describe the major chemical compositions in PM2.5 and their percentage contribution to PM2.5 at the two sites.

It is well known that OC, EC, $SO4^{2-}$, $NO3^{-}$ and $NH4^{+}$ were the dominant chemical components in PM2.5 (Tao et al., 2017). The above-mentioned five major components over the two sites were discussed below based on the results simulated by the Community Multi-scale Air Quality model with the 2D Volatility Basis Set (CMAQ/2D-VBS) (23) at 36- × 36-km resolution with emission inputs derived from a Chinese emission inventory developed and updated to 2015 with details in these studies (Wang et al., 2014; Zhao et al., 2018). The contributors to carbonaceous aerosols in China mainly include coal combustion, vehicle exhaust and biomass burning, etc (Liu et al., 2018).As shown in Fig. 9, the concentrations of OC were significantly higher than that of EC at Qionghai, likely due to the mixed contributions of atmospheric chemical reactions and primary anthropogenic sources to OC (Cao et al., 2004). The nitrate accounted for a large fraction of PM2.5 in Yucheng, it was strongly related to the high emission levels of NH3 and O3 in Yucheng (Wen et al., 2015).

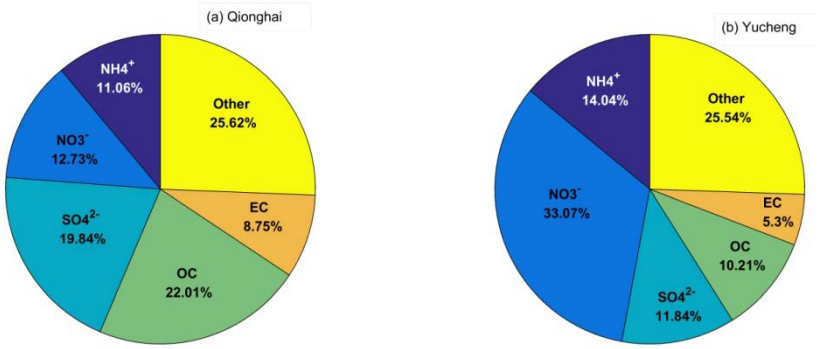

Figure 9: Percentage (%) contribution of $NO3^{-}$, $SO4^{2-}$,$NH4^{+}$,OC and EC to PM2.5 mass in Qionghai (a)and Yucheng (b) in 2015

Section 2.2: Please cite the source for the details given about version 5.0. Comments about expected errors would be useful at this stage.

Response: The non-linear maximum likelihood method used in V5.0 has a strong dependence on the estimation of the first-guess solution. Version 5.0 uses an a priori SDF of a bimodal

log-normal function. The reference 'Hashimoto et al., 2012' gives more details about V5.0. They had performed various test simulations with SKYRAD.pack V4.2 and V5.0 (Hashimoto et al., 2012), and found: In the case of a large amount of coarse particles with radius greater than 10 μm existing , the numerical tests performed by Hashimoto et al showed that V4.2 could retrieve the SDF relatively well, including the coarse mode, in comparison with V5.0, because the smoothness condition given by Eq. (2) allowed the retrieved SDF to be distributed beyond 10 μm radius, on the other hand, V5.0 underestimated the coarse mode of the SDF because of the strong SDF constraint condition given by Eq. (5) with a small model radius rm_2 = 2.0 μm for the coarse mode SDF (Hashimoto et al., 2012). So we have compared the differences between retrieved SSAs at 500 nm byV5.0 and V4.2 when set rm2 = 1.5, 1.8, 2.0(default), 2.5 and 3.0 in Skyrad.pack V5.0 based on the measurements in 2014. As shown in Fig.7, SSAs by V5.0 correlated to SSAs by V4.2 with R= 0.860, 0.837, 0.855, 0.809 and 0.226 when r_{m2} = 1.5, 1.8, 2.5 and 3.0 in V5.0 over Qionghai, respectively. The correlation coefficient between SSA by V5.0 and V4.2 was the highest while setting r_{m2} as 2.0 (the default value) at both the two sites.

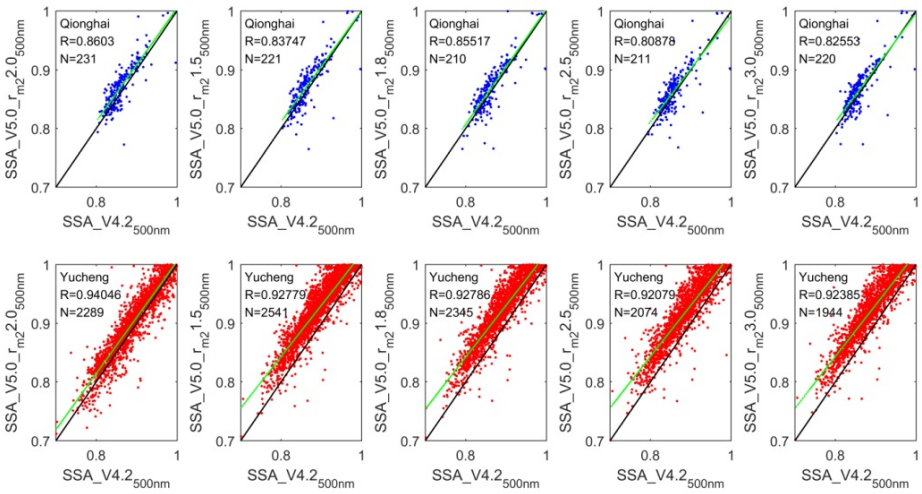

Figure 7: Scattergrams of retrieved SSA between SKYRAD V4.2 and V5.0 when r_{m2} =2.0(default), 1.5, 1.8, 2.5 and 3.0 for Qionghai (a) and Yucheng (b) in 2014.r_{m2} represents the model radius for the coarse mode SDF.

We also investigated whether the total amount of aerosols in the atmosphere were linked to the difference in SSA between the two versions. As shown in Fig. 8, the SSA differences at 500nm between the two versions (defined as: $|SSA\_V5.0_{500nm} - SSA\_V4.2_{500nm}|$) decreased while the corresponding AODs at wavelengths of 500 nm by V5.0 increased at both the two sites. When the

AOD was high (in this study the threshold was set to 0.5 for AOD_{500nm}), SSA retrieved by V5.0 had a good comparison with those with V4.2. It is well known that the inversion products have a very high uncertainty in cases of very low aerosol burdens, the retrieval error in SSA rapidly increases with decreasing AOD (Dubovik et al., 2000), especially in parameters such as the imaginary part of the refractive index.

We have added the above comments and figure in the revised manuscript.

Section 3.1: It is possible to further analyze the comparison of the SDF, including some statistics. In the first part of the paper, perhaps the authors should focus on the analysis of the differences (absolute or relative) and leave the absolute retrievals for the second part of the study (analysis of the aerosol properties). Why AOD is not included in the comparison?

Response: Following the reviewer's suggestion, we have added the following figure which showed the plots of AOD values at each wavelength derived from the solar direct irradiance between the two versions. High correlation was found with a significant coefficient larger than 0.995 at each band except 1020nm over Qionghai. High consistency of AODs between V4.2 and V5.0 indicates that the inversion process in V5.0 did not bring about a large change in the retrieved direct solar radiation (Hashimoto et al., 2012).

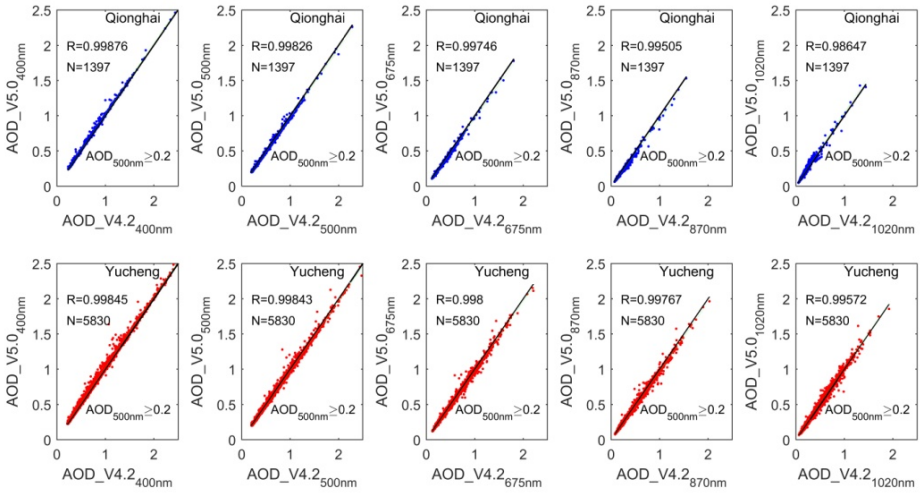

Figure 2: Scatter plot and correspondent linear fitting for the aerosol optical depth (AOD) between SKYRAD V4.2 and V5.0 at wavelengths of 400, 500, 670, 870, and 1020 nm over Qionghai and Yucheng during February 2013 to December 2015.

We have added the above comments and figure in the revised manuscript.

We have replaced Fig.1 with the following figure which shows the retrieved monthly volume size distribution between SKYRAD V4.2 (red lines) and V5.0 (blue lines) for Qionghai (dotted line) and Yucheng (solid lines) during February 2013 to December 2015. As shown in the following figure, V4.2 showed a tri-model pattern with three peak volume at radius of 0.25, 1.16, 11.31 and 0.25, 1.69, 11.31 in July and September over Yucheng, respectively. Figure 3 also showed that there were larger differences in volume SDF of the coarse mode between V4.2 and V5.0 at Qionghai than those at Yucheng in most months.

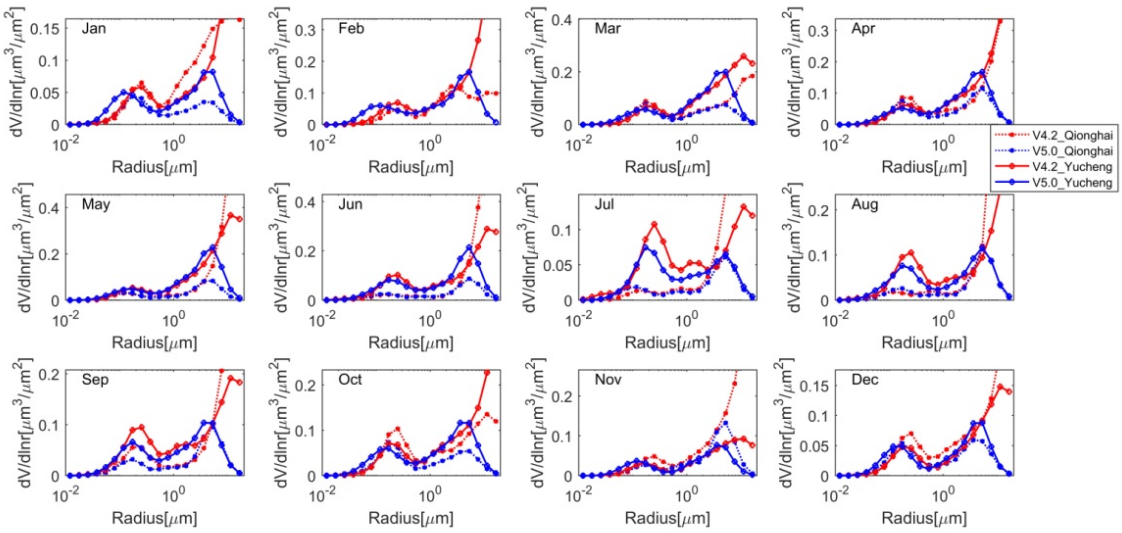

Figure 3: Retrieved monthly volume size distribution between SKYRAD V4.2 (red lines) and V5.0 (blue lines) for Qionghai (dotted line) and Yucheng (solid lines) during February 2013 to December 2015

We have added the above figure and comments in the revised manuscript.

Section 3.2. and 3.3.: similarly to 3.1, concentrate on differences rather than absolute values. Finally, add your opinion about the most adequate version to use in the remaining, based on the results, so both parts of paper are smoothly linked.

Response: Based on the new experiment results as shown in the following figures, the SSA and m_i had relatively high correlation coefficients between V4.2 and V5.0 with default rm_2 value based on the above comparison results. In addition, some tests by Hashimoto et al showed that the SDF setting in V5.0 was useful for detecting ill-conditioned data caused by cirrus contaminations, horizontally and/or temporally inhomogeneous aerosol stratification, and so on (Hashimoto et al., 2012). So we still chose the retrieved results by V5.0 to analyze the seasonal variability of the

aerosol optical properties over Qionghai and Yucheng.

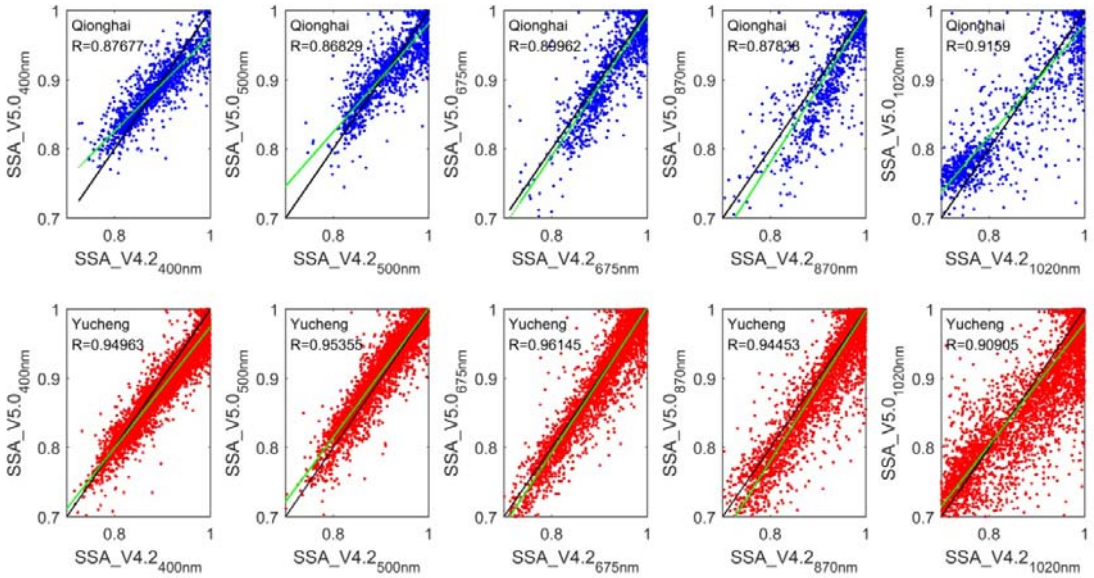

Figure 4: Scattergrams of the single scattering albedo between SKYRAD 4.2 and 5.0 at wavelengths of 400, 500, 670, 870, and 1020 nm over Qionghai and Yucheng during February 2013 to December 2015. Only data with AOD_{500nm}>0.2 are shown. The green line means the fitted linear regression curve.

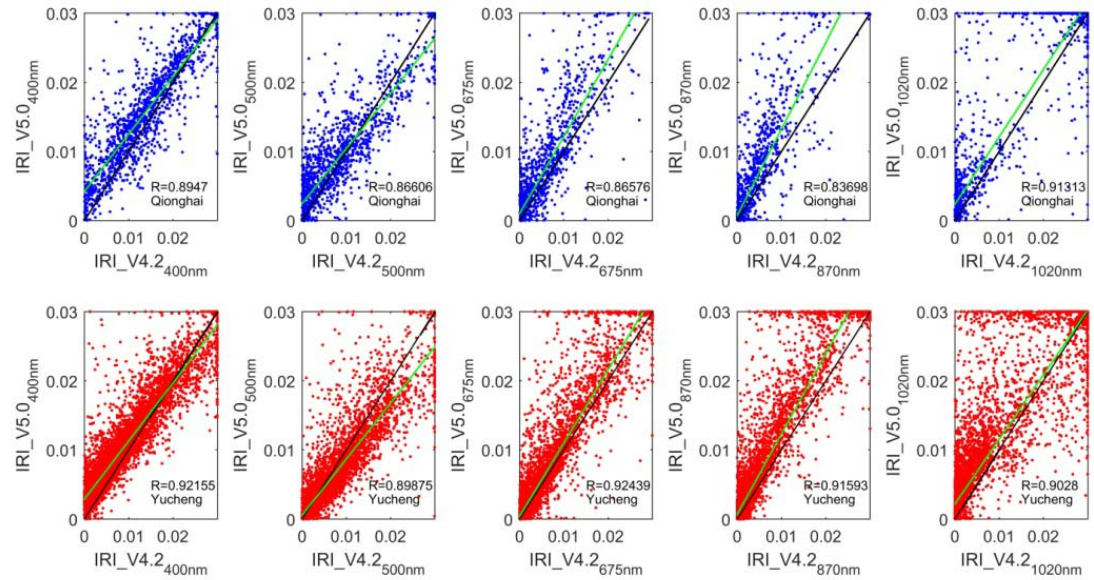

Figure 5: Scattergrams of the imaginary part of the complex refractive index (m_i) results between SKYRAD 4.2 and 5.0 at wavelengths of 400, 500, 670, 870, and 1020 nm over Qionghai and Yucheng during February 2013 to December 2015.

We have added the above comments in the revised manuscript.

Section 3.4: I think the analysis of the aerosol properties at the two sites need a deeper analysis, also including references to previous analysis from China or elsewhere.

Response: Based on the new experiment results, we have made major revision on this section. Section 3.1, 3.2 , 3.3 have been merged into Section 3.1, Section 3.4.1, 3.4.2, 3.4.3, 3.4.4 have been changed into Section 3.2.2, 3.2.3, 3.2.4 , 3.2.5 as follows, Section 3.2.1 is 'The major chemical compositions in PM2.5 at the two sites' as the above, the changes in the manuscript are in red.

3.2.2 AOD

The AOD is representative of the aerosol loading in the atmospheric column and important for the identification of the aerosol source regions and the aerosol evolution.

The AOD showed a distinct seasonal variation over both Qionghai and Yucheng. Figure 5a showed that the seasonal averaged AOD over Qionghai had higher values in spring, winter and autumn while lower in summer. The stable atmospheric circulation provided a stable atmospheric environment background, continuous low-level northeast wind facilitates the transportation of pollutants from the inland to Hainan in spring, winter and autumn (Tang et al., 2019). During summer, the dominant wind is from South to Southeast (Zhu et al., 2005), the main emission source was from the South China Sea and West Pacific, in addition, seasonal upwelling off the east coast of Hainan Island was strongest in summer (Li et al., 2018) which was conducive to pollutant diffusion, meanwhile rich precipitation in summer was effective for eliminating aerosols, so seasonal averaged value of AOD in summer was the lowest in Qionghai. As shown in Figs. 10a, AOD in spring were higher than other seasons. Southerly and northeasterly winds were both prevailing in spring in Qionghai (Liu et al., 2018), long distance transport and emissions from surrounding areas were both the main pollutant sources of Qionghai.

In Yucheng, the AOD averages were commonly higher in summer and spring than in winter and autumn. The humidity of Yucheng (belongs to Shandong province) is highest in summer than other seasons (Meng et al., 2007), the maximum average of 0.99 occurring in summer maybe was caused by hygroscopic effects, high humidity combined with large fractions of hygroscopic chemical components (e.g. sulfate, nitrate, ammonium, and some organic matters) can enhance light extinction and haze intensity the scattering coefficient of secondary inorganic aerosols (such as sulfate, nitrate and ammonium) (Tao et al., 2017). AOD is higher in spring than in autumn and winter likely related to the long-range transportation of dust from northern/northwestern China in spring (Tan et al., 2012).

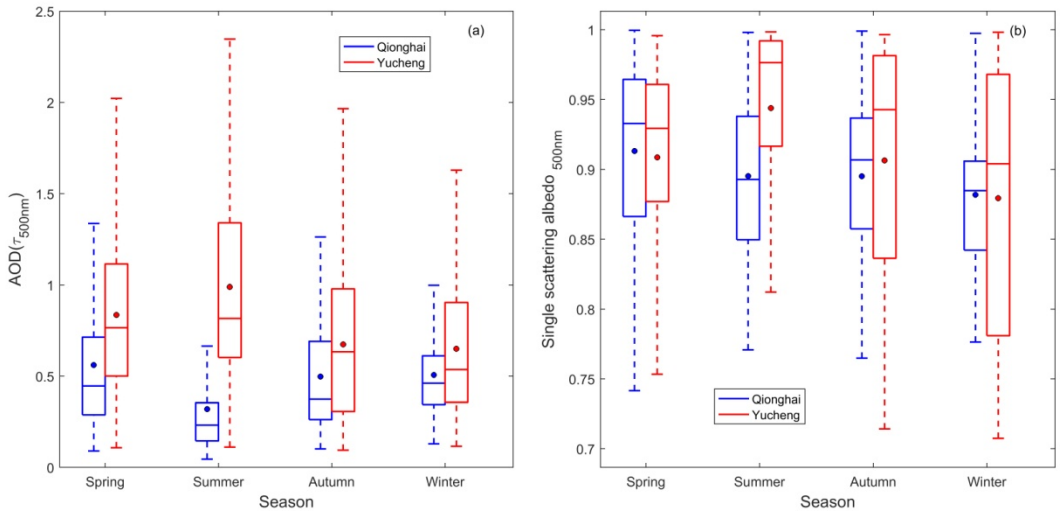

Figure 10: Seasonal variations in the AOD (a) and the single scattering albedo (SSA) (b) based on SKYRAD V5.0 over Qionghai and Yucheng for the period from February 2013 to December 2015. The boxes represent the 25th to 75th percentiles of the distributions while the dots and solid lines within each box represent the means and medians, respectively.

3.2.3 SSA

Figure 10b shows the seasonal averaged SSA at 500 nm for Qionghai and Yucheng during 2013–2015. The seasonal averaged SSA values were approximately 0.91, 0.90, 0.90, and 0.89 in spring, summer, autumn, and winter, respectively. The lowest seasonal average SSA was observed in winter, which was probably attributable to the regional transport of the air masses originated from the regions outside of Hainan province in Eastern China, where a great amount of coal was used for industrial enterprises and emitted high concentrations of OC and EC (Liu et al., 2018). In Yucheng, the seasonal pattern of SSA was consistent with AOD, the lowest seasonal average SSAs were also observed in winter due to carbonaceous aerosols increasing by heating activities and biomass burning, seasonal average contributions of carbonaceous aerosols were evidently higher in cold seasons than in warm seasons (Tao et al., 2017). High concentrations of fine particulate nitrate were frequently observed in summer in Yucheng (Wen et al., 2015), likely to cause the high SSA in summer.

3.2.4 Volume Size Distribution

Figures 11a and b show the seasonal averaged volumes of the different aerosol particle size distributions (dv/dln$r$) in Qionghai and Yucheng. The aerosol volume size distributions were typical bimodal patterns during each season at the Qionghai and Yucheng sites. Figures 6 show that there was a larger contribution of coarse-mode particles to the aerosol volume compared with the fine-mode

particles at the two sites. The fine mode showed a peak at a radius of 0.17 μm in all seasons over Qionghai. The coarse mode was characterized by a peak at a radius of 5.29 μm in spring, summer, and autumn and 3.62 μm in winter. The size distributions showed distinct differences in their dominant modes for the different seasons. As shown in Fig. 11a, the fraction of the fine aerosol particles was much smaller in summer than for the other seasons, the summer meteorological conditions such as high wind speeds, high mixing heights, and the fresh air masses originated from or passed through the sea, which may be contributable to the decrease of pollutant concentrations (Liu et al., 2018) and introducing some sea salt particles of a relatively large size. The seasonal averaged peak of fine mode and coarse mode SDF were both in winter as shown in Fig.11a, the air masses of transport were mainly originated from the mainland China, fine and coarse particle were both long range transported to Qionghai in winter (Wu et al., 2011; Liu et al., 2018).

As shown in Fig. 11b, the coarse-mode particle in Yucheng had a relatively large value compared to the volume distribution of the fine-mode particle. The prevailing winds in Yucheng were from the northwest in winter and spring, Yucheng was in the downwind of Hebei province where located many industrial enterprises emitted pollutants including secondary inorganic aerosols (Tao et al., 2017; Zhao et al., 2018c).The aerosol was not only from winter heating but also from regional transport, the fine-mode and coarse-mode particles was both high in winter in Yucheng. The volume of the coarse aerosol particles relative to the whole was much larger than for the other seasons in spring in Yucheng probably because of the presence of the dust particles transported from the northwest of China and secondary inorganic aerosols emitted from enterprises in Hebei (Tao et al., 2017).

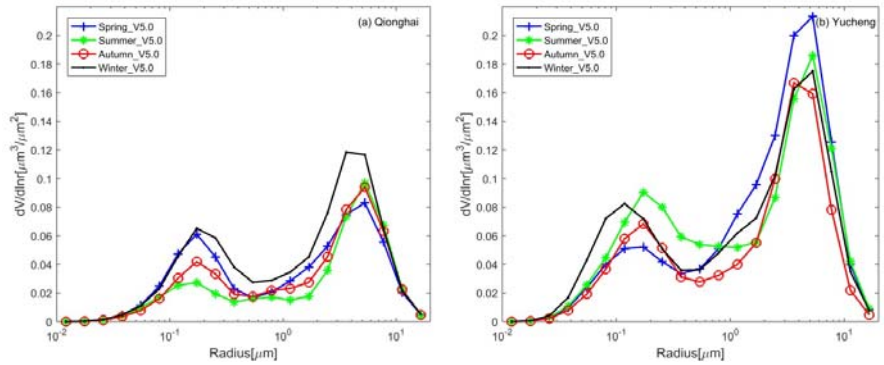

Figure 11: Seasonally averaged volumes of the different aerosol particle size distributions based on SKYRAD V5.0 over Qionghai (a) and Yucheng (b) for the period from February 2013 to December 2015.

3.2.5 Refractive index

Figure 12a showed the seasonal variation of the real part of the refractive index (m_r) at 500 nm over

Qionghai and Yucheng. The averages of m_r at 500 nm in Qionghai were 1.45, 1.46, 1.45, and 1.43 in spring, summer, fall, and winter, respectively. The averages of the real parts were higher in spring compared to the other seasons in Yucheng. The m_r in Yucheng showed a maximum of approximately 1.47 in spring and a minimum of approximately 1.45 in summer.

Figure 12b presented the seasonal variation of the imaginary part of the refractive index at 500 nm over Qionghai and Yucheng. On the contrary to SSA, the results of imaginary part of complex refractive index (m_i) were both highest in winter in the two sites.

Aerosol absorption coefficient was determined by elemental carbon (EC) mass concentration and its coating (Tao et al., 2017), heating activities and biomass burning induced higher carbonaceous aerosols in winter in Yucheng. As shown in Fig.9, OC/EC ratios could be estimated to be greater than 2.0 in Qinghai, suggesting coal and vehicle exhaust as dominant carbonaceous aerosols sources (He et al., 2008; Watson et al., 2001).

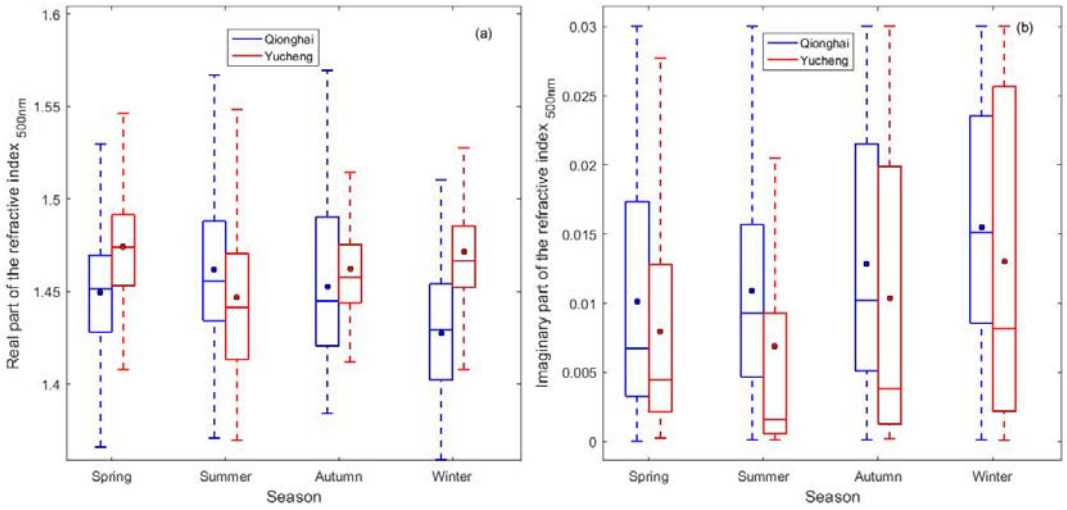

Figure 12: Seasonal variations in the real part of the refractive index (a) and the imaginary part of the refractive index (b) based on SKYRAD V5.0 over Qionghai and Yucheng for the period from February 2013 to December 2015. The boxes represent the 25th to 75th percentiles of the distributions while the dots and solid lines within each box represent the means and medians, respectively.

Line 251 is particularly vague, as other reasons for the increase of AOD in summer are usually considered (differences in transport from remote areas, increase of secondary aerosols due to higher solar radiation...). In contrast to first part of the paper, in the second part I would recommend to focus on the absolute values, represented in monthly means along the year, with

corresponding boxplots, for example. Current analysis based on seasonal averages alone, is not optimum.

Response:

The increase of AOD in summer in Yucheng maybe was caused by hygroscopic effects. Yucheng and the surrounding areas are famous for their agriculture and grazing land. In addition, the site near 20 to 30 km radius located several factories in the production of inorganic and organic fertilizers (Wen et al., 2015), and the application of fertilisers to farmland emitted a great deal of NH3 in summer (Zhao et al., 2012). The humidity of Yucheng (belong to Shandong province) is highest in summer than other seasons (Meng et al., 2007). High humidity combined with large fractions of hygroscopic chemical components can enhance light extinction and haze intensity the scattering coefficient of secondary inorganic aerosols (such as sulfate, nitrate and ammonium) (Tao et al., 2017).

We have tried to represent the monthly means with corresponding boxplots as follows. The references to previous analysis from China or elsewhere related to the two sites are mostly based on seasonal averages. There are no other data available to be inter-compared with our results during the experiment time. To analyze the reasons for the variation or inter-compare based on the references, the temporal variation analysis are based on seasonal averages as above .

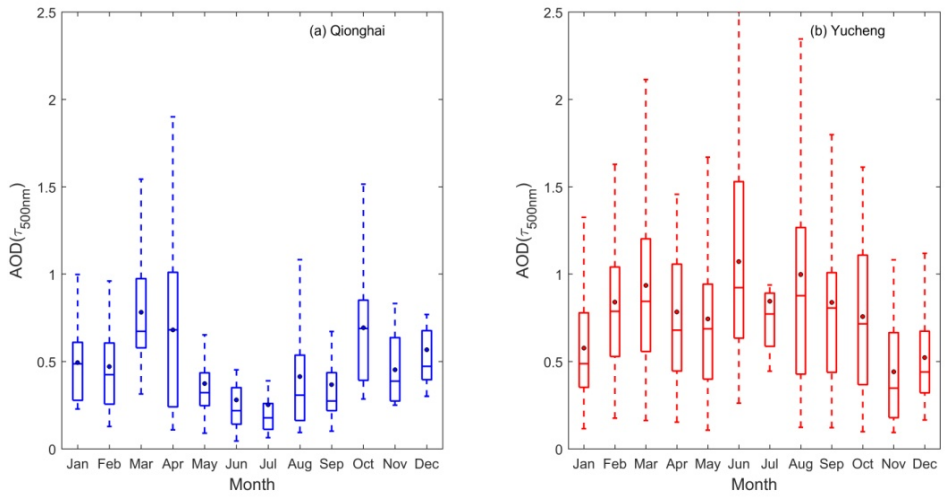

Figure : Monthly variations in the AOD based on SKYRAD V5.0 over Qionghai (a) and Yucheng (b) for the period from February 2013 to December 2015. The boxes represent the 25th to 75th percentiles of the distributions while the dots and solid lines within each box represent the means and medians, respectively.

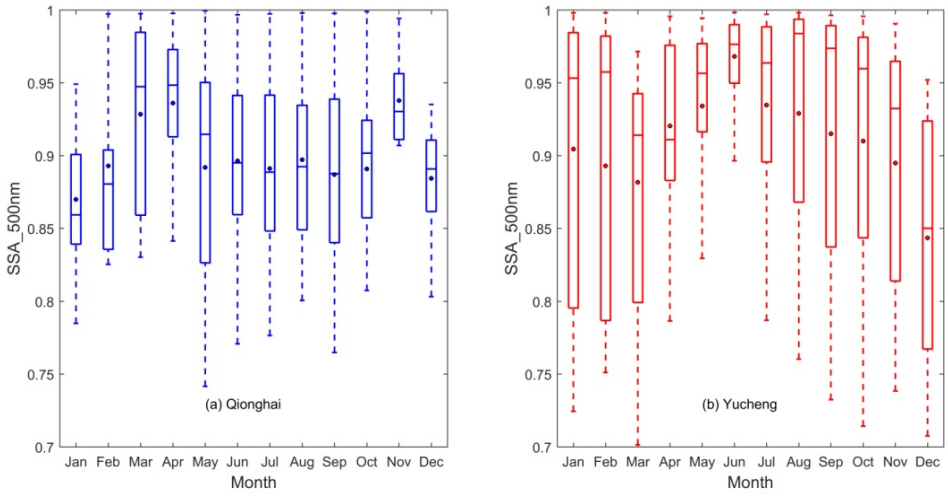

Figure : Monthly variations in the single scattering albedo (SSA) based on SKYRAD V5.0 over Qionghai (a) and Yucheng (b) for the period from February 2013 to December 2015. The boxes represent the 25th to 75th percentiles of the distributions while the dots and solid lines within each box represent the means and medians, respectively.

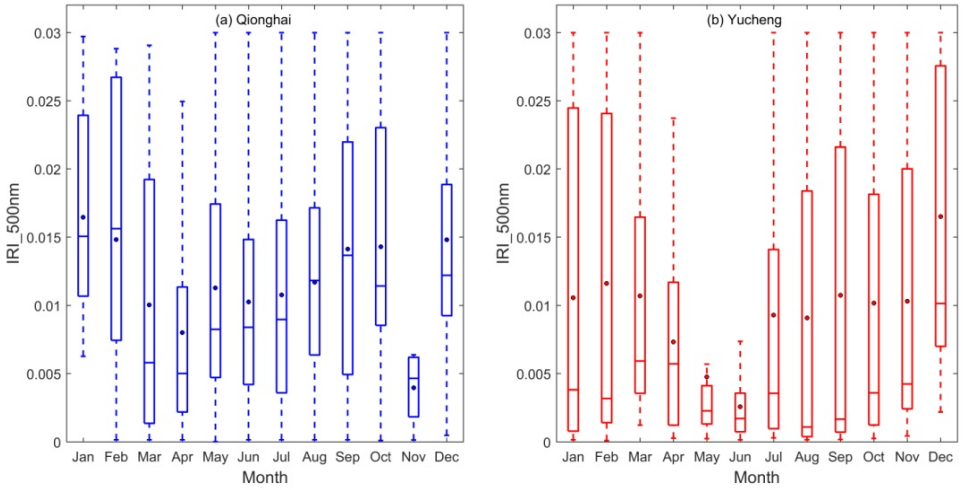

Figure : Monthly variations in the imaginary part of the refractive index based on SKYRAD V5.0 over Qionghai (a) and Yucheng (b) for the period from February 2013 to December 2015. The boxes represent the 25th to 75th percentiles of the distributions while the dots and solid lines within each box represent the means and medians, respectively.

Other specific corrections:

line 59: many -> several? -

Response: We have replaced "many" with "several".

line 74: There are a few -

Response: We have added "a" before "few".

line94: The dynamic range seems should be 10^7 instead of 107? -

Response: We have replaced "107" with "10^7".

line 120-121: rewrite (parenthesis?) -

Response: We missed a right parenthesis. We have added it in the revised manuscript as below.

(i.e., $\ln(r_{i+1}) - \ln(r_i) = \text{const}$)

line 131-132: e^2 -

Response: We have replaced "e2" with "e^2".

line 156: more comments on the cloud screening and quality control -

Response: The standard process of quality control in Skyrad.pack V4.2 and V5.0 applies a retrieval error between observations and calculated theoretical values by using retrieval values, σ_{obs}

$$\sigma_{obs} = \sqrt{W_e \sum_i \left(\frac{\tau_{\lambda_i}}{\tau_{\lambda_i}^{meas}} - 1\right)^2 + W_p \sum_i \sum_j \left[\frac{R_{\lambda_i}(\Theta_j)}{R_{\lambda_i}^{meas}(\Theta_j)} - 1\right]^2}$$

where ($\tau_{\lambda_i}^{meas}$ and $R_{\lambda_i}^{meas}$) and (τ_{λ_i} and R_{λ_i}) are measured and retrieved observation vectors for the AOD and relative sky radiance, N_i , N_j , and $N_{total} = N_i + N_i \times N_j$ indicate the number of measured wavelengths, scattering angles, and their total, respectively, $W_e = W_P = 1/N_{total}$. In V4.2, the data if the value of σ_{obs} is larger than 0.2, but σ_{obs} is set 0.07 as a threshold for data rejection in V5.0. There are some other differences between V4.2 and V5.0 on the issue of quality control of observation data and cloud screening (Hashimoto et al., 2012).

We have added the above comments in the revised manuscript.

line 173: it is important to highlight the fact that the unrealistic coarse mode in v4.2 is removed -

Response: The unrealistic coarse mode in v4.2 is removed in V5.0 by the constraint of a reduced SDF for particles with radius greater than 10 μm. Some tests by Hashimoto et al showed that the SDF setting in V5.0 was useful for detecting ill-conditioned data caused by cirrus contaminations, horizontally and/or temporally inhomogeneous aerosol stratification, and so on (Hashimoto et al., 2012).

We have added the above comments in the revised manuscript.

line 244: The AOD is -

Response: We have replaced "was" with "is".

line 289-291: three significant digits is enough for the refractive index (1.45 etc)

Response: Following the reviewer's suggestion, the numbers referred to the real part of the refractive index in the revise manuscript have been changed to be with three significant digits.

References

Ackerman, A. S., Toon, O. B., Stevens, D. E., Heymsfield, A.J., Ramanathan, V., and Welton E.J.: Reduction of tropical cloudiness by soot, Science, 288, 1042–1047, doi: 10.1126/science.288.5468.1042, 2000.

Bi, J. R., Shi, J. S. , Xie, Y. K., and Liu Y. Z.: Dust Aerosol Characteristics and Shortwave Radiative Impact at a Gobi Desert of Northwest China during the Spring of 2012, J. Meteor. Soc. Japan, 92A, 33–56, doi: 10.2151/jmsj.2014-A03, 2014.

Cai J. X., Guan, Z. Y. , and Ma, F. H. : Possible combined influences of absorbing aerosols and anomalous atmospheric circulation on summertime diurnal temperature range variation over the middle and lower reaches of the Yangtze River, J. Meteor. Res., 30(6), 927–943,doi: 10.1007/s13351-016-6006-1, 2016.

Campanelli, M., Nakajima, T., and Olivieri, B.: Determination of the solar calibration constant for a sun-sky radiometer: Proposal of an in-situ procedure, Appl. Opt., 43, 651–659,

doi:10.1364/AO.43.000651, 2004.

Campanelli, M., Lupi, A., Nakajima, T., Malvestuto, V., Tomasi, C., and Estelles, V.: Summertime columnar content of atmospheric water vapor from ground-based Sun-sky radiometer measurements through a new in situ procedure, J. Geophys. Res., 115, D19304, doi:10.1029/2009JD013211, 2010.

Che, H., Shi, G., Uchiyama, A., Yamazaki, A., Chen, H., Goloub, P., and Zhang, X.: Intercomparison between aerosol optical properties by a PREDE skyradiometer and CIMEL sunphotometer over Beijing, China, Atmos. Chem. Phys., 8, 3199–3214, doi:10.5194/acp-8-3199-2008, 2008.

Che, H. Z., Xia, X. A., Zhu, J., Wang, H., Wang, Y. Q., Sun, J.Y., Zhang, X. C., Zhang, X. Y., and Shi, G. Y.: Aerosol optical properties under the condition of heavy haze over anurban site of Beijing, China, Environ. Sci. Pollut. R., 22, 1043–1053, https://doi.org/10.1007/s11356-014-3415-5, 2014.

Che, H. Z., Qi, B., Zhao, H. J., Xia, X. A., Eck, T. F., Goloub, P., Dubovik, O., Estelles, V., Cuevas-Agulló, E., Blarel, L., Wu, Y. F., Zhu, J., Du, R. G., Wang, Y. Q., Wang, H., Gui, K., Yu, J., Zheng, Y., Sun, T. Z., Chen, Q. L., Shi, G. Y., and Zhang, X. Y..: Aerosol optical properties and direct radiative forcing based on measurements from the China Aerosol Remote Sensing Network (CARSNET) in eastern China, Atmos. Chem. Phys., 18, 405–425, doi:10.5194/acp-18-405-2018, 2018.

Chen, Z., Lu, C. and Fan, L.: Farmland changes and the driving forces in Yucheng, North China Plain. Journal of Geographical Sciences, 22(3), 563-573, 2012.

Dusek, U., Frank, G. P., Hildebrandt, L., Curtius, J., Schneider, J., Walter, S., Chand, D., Drewnick, F., Hings, S., Jung, D., Borrmann, S., and Andreae, M. O.: Size matters more than chemistry for cloud-nucleating ability of aerosol particles, Science, 312(5778), 1375–1378, doi:10.1126/science.1125261, 2006.

Estellés, V., Campanelli, M., Utrillas, M. P., Expósito, F., and Martínez-Lozano, J. A.: Comparison of AERONET and SKYRAD4.2 inversion products retrieved from a Cimel CE318 sunphotometer, Atmos. Meas. Tech., 5, 569–579, https://doi.org/10.5194/amt-5-569-2012, 2012a.

Estellés, V., Smyth, T. J., Campanelli, M.: Columnar aerosol properties in a Northeastern Atlantic site (Plymouth,United Kingdom) by means of ground based skyradiometer data during years 2000-2008, Atmos. Environ., 61, 180–188, doi :10.1016/j.atmosenv.2012.07.024, 2012b.

Hashimoto, M., Nakajima, T., Dubovik, O., Campanelli, M., Che, H., Khatri, P., Takamura, T., and

Pandithurai, G.: Development of a new data-processing method for SKYNET sky radiometer observations, Atmos. Meas. Tech., 5, 2723–2737, https://doi.org/10.5194/amt-5-2723-2012, 2012.

He, L. Y., Hu, M., Zhang, Y. H., Huang, X. F., and Yao, T. T.: Fine particle emissions from on-road vehicles in the Zhujiang Tunnel, China, Environmental Science & Technology, 42, 4461-4466, 2008.

Hensen, J., Sato, M., and Ruedy, R.: Radiative forcing and climate response, J. Geophys. Res., **102**(D6), 6831–6864, doi:10.1029/96JD03436, 1997.

Higurashi, A., Nakajima, T., Holben, B., Smirnov, A., Frouin, R., and Chatenet, B.: A study of global aerosol optical climatology with two channel AVHRR remote sensing, J. Climate, 13, 2011–2027, 2000.

Kaufman, Y. J., Koren, I., Remer, L. A., Rosenfeld, D., and Rudich, Y.: The effect of smoke, dust, and pollution aerosol on shallow cloud development over the Atlantic Ocean, Proc. Natl. Acad. Sci. U.S.A., 102, 11207–11212, doi: 10.1073/pnas.0505191102, 2005.

Kim, D. H., Sohn, B. J., Nakajima, T., Takamura, T., Takemura, T., Choi, B. C., and Yoon, S. C.: Aerosol optical properties over east Asia determined from ground-based sky radiation measurements, J. Geophys. Res., 109, D02209, doi:10.1029/2003JD003387, 2004.

Li, M., Xie, L., Zong, X., Zhang, S., Zhou, L., and Li, J.: The cruise observation of turbulent mixing in the upwelling region east of Hainan Island in the summer of 2012. Acta Oceanologica Sinica, 37(9), 1-12, 2018.

Liu, B., Zhang, J., Wang, L., Liang, D., Cheng, Y., Wu, J., Bi, X., Feng, Y., Zhang, Y., and Yang, H.:Characteristics and sources of the fine carbonaceous aerosols in Haikou, China. Atmospheric Research, 199, 103-112, 2018.

Lu, W., Yang, L., Chen, J., Wang, X., Li, H., Zhu, Y., Wen, L., Xu, C., Zhang, J., Zhu, T. and Wang, W.: Identification of concentrations and sources of PM 2.5-bound PAHs in North China during haze episodes in 2013. Air Quality, Atmosphere & Health, 9(7), 823-833, 2016.

Meng, C. L., and Xu, Z. X.: Relation between ENSO and Precipitation in Shandong . Yellow River, 1, 2007 (in Chinese).

Nakajima, T., Tanaka, M., and Yamauchi, T.: Retrieval of the optical properties of aerosols from the aureole and extinction data, Appl. Optics, 22, 2951–2959, doi: 10.1364/AO.22.002951, 1983.

Nakajima, T. and Tanaka, M.: Algorithms for radiative intensity calculations in moderately thick

atmospheres using a truncation approximation, J. Quant. Spectrosc. Ra., 40, 51–69, doi: 10.1016/0022-4073(88)90031-3, 1988.

Nakajima, T., Tonna, G., Rao, R., Kaufman, Y., and Holben, B.: Use of sky brightness measurements from ground for remote sensing of particulate polydispersions. Appl. Optics, 35, 2672–2686, doi: 10.1364/AO.35.002672, 1996.

Nakajima, T., Yoon, S. C., Ramanathan, V., Shi, G. Y., Takemura, T., Higurashi, A., Takamura, T., Aoki, K., Sohn, B. J., Kim, S. W., Tsuruta, H., Sugimoto, N., Shimizu, A., Tanimoto, H., Sawa, Y., Lin, N. H., Lee, C. T., Goto, D., and Schutgens, N.: Overview of the Atmospheric Brown Cloud East Asian Regional Experiment 2005 and a study of the aerosol direct radiative forcing in east Asia, J. Geophys. Res., 112, D24S91, doi:10.1029/2007JD009009, 2007.

Peel, M. C. and Finlayson, B. L. and McMahon, T. A.: Updated Asian map of the Köppen climate classification system. Hydrol. Earth Syst. Sci. 11: 1633-1644, 2007.

Phillips, B. L.: A technique for numerical solution of certain integral equation of first kind, J. Assoc. Comput. Mach., 9, 84–97, 1962.

Pope lii, C.A., Burnett, R.T., Thun, M. J., Calle, E. E., Krewski, D., Ito, K., and Thurston, G. D.: Lung cancer, cardiopulmonary mortality, and long-term exposure to fine particulate air pollution, J. Am. Med. Assoc, 287(9), 1132–1141, doi: 10.1001/jama.287.9.1132, 2002.

Ramanathan, V., Crutzen, P. J., Kiehl, J. T., Rosenfeld, D.: Aerosols, climate, and the hydrological cycle, Science, 294, 2119–2124, 2001.

Rodgers, C. D.: Inverse Method for Atmospheric Sounding, World Sci., Singapore, 240, 2000.

Samet, J.M., Zeger, S.L., Dominici, F., Coursac, I., Dockery, D.W., Schwartz, J., and Zanobetti, A.: The national morbidity, mortality, and air pollution study. Part II: morbidity and mortality from air pollution in the United States, Health Effects Institute, Cambridge MA, Research Report 94, 2000.

Sun, K., Liu, H. N., Wang, X. Y., Peng, Z., and Xiong, Z.: The aerosol radiative effect on a severe haze episode in the Yangtze River Delta., J. Meteor. Res., 31(5), 865–873, doi: 10.1007/s13351-017-7007-4, 2017.

Takamura, T., and Nakajima, T.: Overview of SKYNET and its activities, Opt. Pura Y Apl., 37, 3303–3308, 2004.

Tan, S. C., Shi, G. Y., and Wang, H.: Long-range transport of spring dust storms in Inner Mongolia and impact on the China seas. Atmospheric Environment, 46, 299-308, 2012.

Tang, J.X., Fu, C. B., Dan, L., Lin X. B.: Analysis on potential sources of air pollutants in Hainan during haze pollution. Environmental Science and Management, 06, 2019 (in Chinese).

Tao, J., Zhang, L., Cao, J., and Zhang, R.:A review of current knowledge concerning PM 2. 5 chemical composition, aerosol optical properties and their relationships across China. Atmospheric Chemistry and Physics, 17(15), 9485-9518, 2017.

Twomey, S.: On the numerical solution of Fredholm integral equations of the first kind by the inversion of the linear system produced by quadrature, J. Assoc. Comput. Mach., 10, 97–101, 1963.

Turchin, V. F. and Nozik, V. Z. : Statistical regularization of the solution of incorrectly posed problems, Izv. Atmos. Ocean. Phy.+, **5**, 14–18, 1969.

Uchiyama, A., Yamazaki, A., Togawa, H., and Asano, J.: Characteristics of Aeolian dust observed by sky-radiometer in the Intensive Observation Period 1 (IOP1), J. Meteor. Soc. Japan, 83A, 291–305, doi: 10.2151/jmsj.83A.291, 2005.

Wang, S. X., Zhao, B., Cai, S. Y., Klimont, Z., Nielsen, C. P., Morikawa, T., Woo, J. H., Kim, Y., Fu, X., Xu, J. Y., Hao, J. M., and He, K. B.: Emission trends and mitigation options for air pollutants in East Asia. Atmospheric Chemistry and Physics, 14(13), 6571-6603, 2014.

Wang, Z. W., Yang, S. Q., Zeng, Q. L., and Wang, Y. Q.: Retrieval of aerosol optical depth for Chongqing using the HJ-1 satellite data, J. Meteor. Res., 31(3), 586 – 596, doi: 10.1007/s13351-017-6102-x, 2017.

Wang, Z. Z., Liu, D., Wang, Z., Wang, Y. J., and Khatri, P.: Seasonal characteristics of aerosol optical properties at the SKYNET Hefei site (31.90°N, 117.17°E) from 2007 to 2013, J. Geophys. Res., 119, 6128–6139, doi:10.1002/2014JD021500, 2014.

Wen, L., Chen, J.M., Yang, L.X., Wang, X.F., Xu, C.H., Sui, X., Yao, L., Zhu, Y.H., Zhang, J.M., Zhu, T., and Wang, W.X.: Enhanced formation of fine particulate nitrate at a rural site on the North China Plain in summer: The important roles of ammonia and ozone, Atmospheric Environment, 101, 294-302, 2015.

Wu, D., Wu, C., Li, F., and Chen, H.: Air pollution episode in southern China due to the long range transport of coarse particle aerosol. China Environmental Science, 31(4), 540-545, 2011(in Chinese).

Yang, Y. R., Liu, X. G., Qu, Y., An, J. L., Jiang, R., Zhang, Y. H., Sun, Y. L., Wu, Z. J., Zhang, F., Xu, W. Q., and Ma, Q. X.: Characteristics and formation mechanism of continuous hazes in China: A case study during the autumn of 2014 in the North China Plain, Atmos.Chem. Phys., 15,

8165-8178, doi: 10.5194/acp-15-8165-2015, 2015.

Yin, Y., Zhu, D., Tang, W.W., Martini I. P.: The application of GPR to barrier-lagoon sedimentation study in Boao of Hainan Island. Journal of Geographical Sciences, 12(3), 313-320, 2002.

Zhao, B., Wang, P., Ma, J.Z., Zhu, S., Pozzer, A., and Li, W.: A high-resolution emission inventory of primary pollutants for the Huabei region, China. Atmos.Chem. Phys., 12, 481-501, 2012.

Zhao, B., Liou, K.-N., Gu, Y., Jiang, J. H., Li, Q., Fu, R., Huang, L., Liu, X., Shi, X., Su, H., and He, C.: Impact of aerosols on ice crystal size, Atmos. Chem. Phys., 18, 1065-1078, DOI 10.5194/acp-18-1065-2018, 2018a.

Zhao, B., Zheng, H., Wang, S., Smith, K. R., Lu, X., Aunan, K., Gu, Y., Wang, Y., Ding, D., Xing, J., Fu, X., Yang, X. D., Liou, K. N., and Hao, J.M.: Change in household fuels dominates the decrease in PM2. 5 exposure and premature mortality in China in 2005–2015. Proceedings of the National Academy of Sciences, 115(49), 12401-12406, 2018b.

Zhao, B., Jiang, J. H., Diner, D. J., Su, H., Gu, Y., Liou, K.-N., Jiang, Z., Huang, L., Takano, Y., Fan, X.H., and Omar, A. H.: Intra-annual variations of regional aerosol optical depth, vertical distribution, and particle types from multiple satellite and ground-based observational datasets, Atmos. Chem. Phys., 18, 11247–11260, doi:10.5194/acp-18-11247-2018, 2018c.

Zhu, D., Yin, Y., Martini, I. P.: Geomorphology of the Boao coastal system and potential effects of human activities - Hainan Island, South China. Journal of Geographical Sciences, 15(2):187-198, 2005.